
Differentially Private Gradient Flow based on the Sliced Wasserstein Distance for Non-Parametric Generative Modeling

Ilana Sebag
Criteo AI Lab, Dauphine-PSL

Muni Sreenivas PYDI
Dauphine-PSL

Jean-Yves Franceschi
Criteo AI Lab

Alain Rakotomamonjy
Criteo AI Lab

Mike Gartrell
Criteo AI Lab

Jamal Atif
Dauphine-PSL

Alexandre Allauzen
Dauphine-PSL

Abstract

Safeguarding privacy in sensitive training data is paramount, particularly in the context of generative modeling. This is done through either differentially private stochastic gradient descent, or with a differentially private metric for training models or generators. In this paper, we introduce a novel differentially private generative modeling approach based on parameter-free gradient flows in the space of probability measures. The proposed algorithm is a new discretized flow which operates through a particle scheme, utilizing drift derived from the sliced Wasserstein distance and computed in a private manner. Our experiments show that compared to a generator-based model, our proposed model can generate higher-fidelity data at a low privacy budget, offering a viable alternative to generator-based approaches.

1 INTRODUCTION

With the use of deep learning in critical applications (Aggarwal et al., 2021; Shen et al., 2017), there is an increasing awareness of its limitations, especially in the realm of privacy. Numerous privacy attacks have been demonstrated on machine learning algorithms, where the membership of specific data points in the training set has been exposed (Shokri et al., 2017; Hu et al., 2022), and worse still, approximate versions of some data points have been reconstructed by merely exposing

the parameters of a learned model (Lacharité et al., 2018; Mai et al., 2018). Deep-learning-based generative models are no exception to this trend of privacy attacks (Chen et al., 2020b; Carlini et al., 2023).

One of the main solutions to the problem of privacy attacks is differential privacy (DP), a rigorous framework that preserves training data privacy (Dwork et al., 2006; Dwork, 2011; Dwork & Roth, 2014). DP ensures that a single data point’s inclusion or exclusion minimally affects analysis outcomes. For deep-learning-based approaches, this is typically achieved by adding calibrated noise to the gradient steps that involve the use of sensitive training data, with differentially private stochastic gradient descent (DP-SGD, Abadi et al., 2016) being the prototypical example.

While extensively studied in classification contexts, the application of differential privacy in generative models remains a nascent area of research. For generative modeling, privacy protection for sensitive training data is achieved through two main approaches. The first involves utilizing variants of DP-SGD for training standard generative models (Xie et al., 2018; Chen et al., 2020a; Long et al., 2021; Dockhorn et al., 2023; Ghalebikesabi et al., 2023); either in the context of generator learning (Cao et al., 2021) or diffusion models (Dockhorn et al., 2023). The second method employs differentially private metrics (Harder et al., 2021; Rakotomamonjy & Ralaivola, 2021; Harder et al., 2023) as losses for training generators.

In this paper, we take a different approach to DP generative modeling that is based on gradient flows. We model a target distribution by analyzing a functional of the following type, on the space of probability measures:

$$\min_{\mu \in \mathcal{P}(\Omega)} \text{PrivateCost}_\sigma(\mu, \nu) + \lambda \text{Reg}(\mu), \quad (1)$$

where ν is the probability measure to be modeled, $\text{PrivateCost}_\sigma$ is a cost functional on the space of proba-

bility measures $\mathcal{P}(\Omega)$ that can be computed in a private manner, and Reg is a regularization functional that prevents overfitting to training samples. Under assumptions of regularity, we show in Section 2.3 that problem (1) admits a *gradient flow* where a solution can be obtained by making μ evolve according to a partial differential equation (PDE) of the following type:

$$\frac{\partial \rho_t}{\partial t} = -\text{div}(v_t^{(\sigma)} \rho_t) + \lambda \Delta \rho_t, \quad (2)$$

where ρ_t is the density of the probability flow $(\mu_t)_{t \geq 0}$ at time t , and $v_t^{(\sigma)}$ is a drift term that can be estimated privately.

Gradient flows have a rich theoretical background (Ambrosio, 2008; Santambrogio, 2016) and have found applications in diverse fields such as cosmology (Brenier et al., 2003), fluid dynamics (Benamou & Brenier, 2000), and atmospheric science (Cullen, 2006). Their application to generative modeling is relatively recent and still in its early stages. Among others, Liutkus et al. (2019) propose a non-parametric generative modeling approach that is based on the gradient flow of the sliced Wasserstein distance (SWD). In this approach, samples are drawn from an initial distribution, and then evolve according to a PDE that dictates the gradient flow. Bonet et al. (2022) use a similar idea, but the flow is a numerically approximated Jordan–Kinderlehrer–Otto (JKO) type scheme. However, privacy was not a consideration in these works. Subsequently, Rakotomamonjy & Ralaivola (2021) propose a private version of SWD that can be used to train generative models, however it was not known if this private-distance admits a gradient flow. This motivates the following question:

Can we develop a principled formalism for privacy-preserving generative modeling through gradient flows?

In this paper, we provide an affirmative response to this question by relying on two theoretically grounded frameworks: differential privacy, and gradient flows on probability spaces. Our contributions are the following.

- We introduce a novel theoretically-grounded algorithm for differentially private generative modeling rooted in gradient flows in the Wasserstein space. Our algorithm is the discretization of an evolution equation of the type shown in (2). Furthermore, we prove that the evolution is the gradient flow of a functional of the form (1), where the PrivateCost is based on a differentially private SWD of Rakotomamonjy & Ralaivola (2021).
- We give a rigorous differential privacy guarantee for our algorithm by careful tracking of the parameters of the discretized flow.

- Through experiments, we confirm the practical viability of our proposed algorithm compared to baseline models that are generator-based.

The novelty and performance of our approach establish a promising foundation for future research in the field of private generative modeling.

Notations. Throughout the paper we use Ω to denote the sample space. We assume that Ω is a compact subset of \mathbb{R}^d . For any subset $\mathcal{A} \subseteq \mathbb{R}^d$, we use $\mathcal{P}(\mathcal{A})$ to denote the set of probability measures supported on \mathcal{A} equipped with the Borel σ -algebra. For $\mu, \nu \in \mathcal{P}(\Omega)$, we use $\Pi(\mu, \nu) \subseteq \mathcal{P}(\Omega^2)$ to denote the set of joint distributions or “couplings” between μ and ν . For $\mu \in \mathcal{P}(\Omega)$ and a measurable function $M: \Omega \rightarrow \Omega$, the push-forward operator $\#$ defines a probability measure $M_{\#}\mu \in \mathcal{P}(\Omega)$ such that $M_{\#}\mu(A) = \mu(M^{-1}(A))$ for all measurable $A \subseteq \Omega$. For $r > 0$, we use $\bar{B}(0, r)$ to denote a closed ball of radius r .

2 BACKGROUND

In this section, we introduce the core principles of three key areas that form the foundation of our method: differential privacy, optimal transport, and gradient flows.

2.1 Differential Privacy

Definition 1. A random mechanism $\mathcal{M}: \mathcal{D} \rightarrow \mathcal{R}$ is (ϵ, δ) -DP if for any two adjacent inputs $d_1, d_2 \in \mathcal{D}$ and any subset of outputs $\mathcal{S} \subseteq \mathcal{R}$,

$$\mathbb{P}[\mathcal{M}(d_1) \in \mathcal{S}] \leq e^\epsilon \mathbb{P}[\mathcal{M}(d_2) \in \mathcal{S}] + \delta. \quad (3)$$

A mechanism that is $(\epsilon, 0)$ -DP is said to be ϵ -pure DP. $\delta > 0$ allows for the ϵ -pure DP condition to be broken with probability at most δ . Notice that adjacent inputs refer to two datasets differing only by a single example.

A classical example of a DP mechanism is the Gaussian mechanism that operates on a function $f: \mathcal{D} \rightarrow \mathbb{R}^d$ as

$$\mathcal{M}_f(d) = f(d) + \mathcal{N}(0, \sigma^2 \mathcal{I}_d). \quad (4)$$

Define the ℓ_2 sensitivity of f as $\Delta_2(f) := \max_{d_1, d_2: \text{adjacent} \in \mathcal{D}} \|f(d_1) - f(d_2)\|_2$. For $c^2 > 2 \ln(1.25/\delta)$ and $\sigma \geq c \frac{\Delta_2(f)}{\epsilon}$, the Gaussian mechanism is (ϵ, δ) -DP (Dwork & Roth, 2014).

2.2 Optimal Transport

The p -Wasserstein distance between two probability measures $\mu, \nu \in \mathcal{P}(\Omega)$ is defined as

$$\mathcal{W}_p(\mu, \nu) = \left(\inf_{\pi \in \Pi(\mu, \nu)} \int_{\Omega^2} \|x - y\|_2^p d\pi(x, y) \right)^{\frac{1}{p}}. \quad (5)$$

For $p = 2$, i.e., for the squared Euclidean cost, a celebrated result of Brenier (1991) proves that the optimal way to transport mass from μ to ν is through a measure-preserving transport map $M: \Omega \rightarrow \Omega$ of the form $M(x) = x - \nabla\psi(x)$, where $\psi: \Omega \rightarrow \mathbb{R}$ is a convex function termed the Kantorovich potential between μ and ν . In the one-dimensional case, the optimal transport map has a closed-form expression given by

$$M(x) = F_\nu^{-1} \circ F_\mu(x), \quad (6)$$

where F_μ and F_ν are the cumulative distribution functions (CDFs) of μ and ν , respectively. In higher dimensions, no such closed form exists. For more general costs, optimal transportation may not even be achieved by a deterministic transport map, as opposed to a probabilistic transport plan.

The sliced Wasserstein distance (SWD) takes advantage of the simplicity of OT in one-dimension by computing a distance between $\mu, \nu \in \mathcal{P}(\Omega)$ through their projections $P_\#^\theta \mu, P_\#^\theta \nu \in \mathcal{P}(\mathbb{R})$ onto the unit sphere $\mathbb{S}^{d-1} = \{\theta \in \mathbb{R}^d \mid \|\theta\|_2 = 1\}$. Here $P^\theta: \Omega \rightarrow \mathbb{R}$ denotes the projection operator defined as $P^\theta(x) = \langle x, \theta \rangle$. Formally,

$$\mathcal{SW}_2^2(\mu, \nu) = \int_{\mathbb{S}^{d-1}} \mathcal{W}_2^2(P_\#^\theta \mu, P_\#^\theta \nu) d\theta, \quad (7)$$

where $d\theta$ is the uniform probability measure on \mathbb{S}^{d-1} . Like \mathcal{W}_2 , the \mathcal{SW}_2 also defines a metric on $\mathcal{P}(\Omega)$.

2.3 Gradient Flows

The gradient flow of a differentiable function $F: \mathbb{R}^d \rightarrow \mathbb{R}$ is a continuous trajectory $x: [0, T] \rightarrow \mathbb{R}^d$ that is a solution to the Cauchy problem given by $x'(t) = -\nabla F(x(t))$ with some initialization $x(0) = x_0$.

Intuitively, gradient flow of F is a curve of steepest descent of F .

A discrete approximation to this flow using explicit Euler scheme gives the gradient descent algorithm for minimizing F . If F is not smooth, we may still discretize the gradient flow through the implicit Euler scheme given by

$$x_{k+1}^h \in \arg \min_{x \in \mathbb{R}^d} F(x) + \frac{\|x - x_k^h\|^2}{2h}, \quad (8)$$

where $h > 0$ denotes the step size. For a functional $\mathcal{F}: \mathcal{P}(\Omega) \rightarrow \mathbb{R}$ defined on the Wasserstein space $(\mathcal{P}(\Omega), \mathcal{W}_2)$, we can propose a discrete gradient flow analogous to (8):

$$\mu_{k+1}^h \in \arg \min_{\mu \in \mathcal{P}(\Omega)} \mathcal{F}(\mu) + \frac{\mathcal{W}_2^2(\mu, \mu_k^h)}{2h}.$$

For “nice” functionals \mathcal{F} , a continuous version of the above discretization is well-defined, and may reduce to a flow dictated by a PDE. A classical example is the Fokker-Plank PDE given by

$$\frac{\partial \rho_t}{\partial t} = \operatorname{div}(\rho_t \nabla V) + \lambda \Delta \rho_t, \quad (9)$$

which is the gradient flow of the following functional:

$$\mathcal{F}(\mu) = \int_{\Omega} V d\mu + \lambda \mathcal{H}(\mu), \quad (10)$$

where V is a potential function, $\lambda > 0$ is a constant, and \mathcal{H} denotes the negative entropy functional, defined as $\mathcal{H}(\mu) := \int_{\Omega} \rho(x) \log \rho(x) dx$ if μ admits a density ρ and $\mathcal{H}(\mu) = +\infty$ otherwise.

3 RELATED WORK

Optimal transport for generative modeling. Arjovsky et al. (2017) uses GAN architecture to minimize \mathcal{W}_1 between source and target, where the discriminator learns the Kantorovich potential in the dual form of \mathcal{W}_1 . Similarly, Bousquet et al. (2017) minimize \mathcal{W}_1 , but using its primal form, inspired by variational auto-encoders (VAEs). See Genevay et al. (2017) for a nice discussion. Genevay et al. (2018) uses entropy-regularized OT distances. Salimans et al. (2016) uses some OT-based distance called energy distance for training GANs.

The closest work to ours is Liutkus et al. (2019), who propose a gradient flow based generative model that minimizes a function of the type of Equation (1) where the cost function is \mathcal{SW}_2 . The gradient flow is then simulated with a particle-scheme. Bonet et al. (2022) use the same functional as Liutkus, but they use a JKO scheme for the flow instead of a particle approach.

Differentially private optimal transport. There is surprisingly little work on defining rigorous OT metrics that can be computed in a private manner, and thus little for the many ML algorithms that use OT to draw from regarding privacy. Lê Tien et al. (2019) use random projections to make \mathcal{W}_1 computation differentially private for the purpose of domain adaptation, but do not analyze the resulting distance theoretically. Rakotomamonjy & Ralaivola (2021) is the first to rigorously present a Gaussian smoothed version of \mathcal{SW}_2 defined as

$$\mathcal{G}_\sigma \mathcal{SW}_2^2(\mu, \nu) = \int_{\mathbb{S}^{d-1}} \mathcal{W}_2^2(P_\#^\theta \mu * \xi_\sigma, P_\#^\theta \nu * \xi_\sigma) \alpha(\theta) d\theta, \quad (11)$$

where $\xi_\sigma \sim \mathcal{N}(0, \sigma^2)$. They show that this distance and some extensions (Rakotomamonjy et al., 2021)

are inherently differentially private, as the smoothing acts as a Gaussian mechanism. This allows them to seamlessly integrate a differentially private loss function into machine learning problems that involve comparing distributions, such as domain adaptation and generator-based generative modeling.

Differentially private generative modeling. Several recent articles have proposed DP generative modeling. Most of them are based on DP-SGD either in the context of generator learning (Cao et al., 2021) or diffusion models (Dockhorn et al., 2023). Few works learn generators by optimizing a naturally DP loss (Rakotomamonjy & Ralaivola, 2021; Harder et al., 2021, 2023). Here, we go beyond in this last trend by introducing a theoretically sound gradient flow of a differentially private loss function, which relies on Gaussian-smoothed SWD for scalability purpose.

4 DIFFERENTIALLY PRIVATE GRADIENT FLOW

In this section, we present the theoretical building blocks of our method. In Section 4.1, we present the gradient flow of a functional based on the Gaussian-smoothed sliced-Wasserstein distance of Rakotomamonjy & Ralaivola (2021) defined in Equation (11). In Section 4.2, we present a particle scheme to simulate the discretization of this flow, borrowing from the method of Liutkus et al. (2019). Finally in Section 4.3, we present the DP guarantee for the resulting method.

4.1 Gradient Flow of $\mathcal{G}_\sigma \mathcal{SW}_2$

We study the following functional over the Wasserstein space $(\mathcal{P}(\Omega), \mathcal{W}_2)$:

$$\mathcal{F}_{\lambda, \sigma}^\nu(\mu) = \frac{1}{2} \mathcal{G}_\sigma \mathcal{SW}_2^2(\mu, \nu) + \lambda \mathcal{H}(\mu), \quad (12)$$

where $\nu \in \mathcal{P}(\Omega)$ is the target distribution to be modeled, $\lambda > 0$ signifies the strength of the entropic regularization and $\sigma > 0$ signifies the smoothing of the probability measures in the inner optimal transport problem in $\mathcal{G}_\sigma \mathcal{SW}_2$. In Section 4.3, we show how σ relates to the privacy parameters (ε, δ) in the discretized flow.

The following theorem gives the continuity equation for the gradient flow of the functional in (12).

Theorem 1. *Let $\nu \in \mathcal{P}(\overline{B}(0, r))$ have a strictly positive smooth density. For $\lambda > 0$ and $r > \sqrt{d}$, let the starting distribution $\mu_0 \in \mathcal{P}(\overline{B}(0, r))$ have a density $\rho_0 \in L^\infty(\overline{B}(0, 1))$. There exists a minimizing movement scheme $(\mu_t)_{t \geq 0}$ associated with Equation (12). Further, $(\mu_t)_{t \geq 0}$ admits densities $(\rho_t)_{t \geq 0}$ that satisfy the following continuity equation:*

$$\frac{\partial \rho_t}{\partial t} = -\operatorname{div}(v_t^{(\sigma)} \rho_t) + \lambda \Delta \rho_t, \quad (13)$$

with:

$$v_t^{(\sigma)}(x) = v^{(\sigma)}(x, \mu_t) = \int_{\mathbb{S}^{d-1}} (\psi_{t, \theta}^{(\sigma)})'(\langle x, \theta \rangle) \theta \, d\theta, \quad (14)$$

where $\psi_{t, \theta}^{(\sigma)}$ is the Kantorovich potential between $P_{\#}^\theta \mu_t * \xi_\sigma$ and $P_{\#}^\theta \nu * \xi_\sigma$ with $\xi_\sigma \sim \mathcal{N}(0, \sigma^2)$.

It is instructive to consider the following special cases over the (λ, σ) parameter landscape.

- (Pure \mathcal{SW}_2 Flow) $\lambda = 0, \sigma \rightarrow 0$. In this regime, we recover the pure \mathcal{SW}_2 flow first studied by Bonnotte (2013). The discretization of this flow is not differentially private. Moreover, as noted in Liutkus et al. (2019), an unregularized flow is not suitable for generative modeling purposes, as the entropy term injects randomness and ensures that the flow is “sufficiently expressive”.
- (Entropic \mathcal{SW}_2 Flow) $\lambda > 0, \sigma \rightarrow 0$. In this regime, we recover the entropic regularized \mathcal{SW}_2 flow first studied by Liutkus et al. (2019). Although Liutkus et al. (2019) use a discretization of this flow for generative modeling, it is not differentially private.
- (Heat Flow) $\lambda > 0, \sigma \rightarrow \infty$ or $\lambda \rightarrow \infty, \sigma > 0$. As $\sigma \rightarrow \infty$,

$\mathcal{G}_\sigma \mathcal{SW}_2(\mu, \nu) \rightarrow 0$ and by rescaling time as $t' = t/\lambda$, we recover the classical heat equation:

$$\frac{\partial \rho_t}{\partial t} = \Delta \rho_t. \quad (15)$$

As $\lambda \rightarrow \infty$, we again recover the heat equation in (15), as the entropy term dominates.

- ($\mathcal{G}_\sigma \mathcal{SW}_2$ Flow) $\lambda \geq 0, \sigma > 0$. To the best of our knowledge, we are the first to analyze this regime. As with the pure \mathcal{SW}_2 flow, $\lambda = 0$ is unsuitable for generative modeling.

The proof of Theorem 1 is based on prior proofs of Bonnotte (2013) and Liutkus et al. (2019). It introduces two key elements of novelty: (1) existence and regularity of solutions to the minimization of $\mathcal{F}_{\lambda, \sigma}^\nu(\mu)$, and (2) analysis of the first variation (akin to a derivative) of the squared Gaussian-smoothed \mathcal{SW}_2 metric.

4.2 Particle Scheme for Discretized Flow

From Equation (13) we observe that the gradient flow of $\mathcal{G}_\sigma \mathcal{SW}_2$ corresponds to a nonlinear Fokker-Plank

type equation, where the drift term is dependent on the density of the solution. This is caused by the dependency of $v_t^{(\sigma)}$ on the Kantorovich potential $\psi_{t,\theta}^{(\sigma)}$, which is dependent on the smoothed projection of μ_t along θ i.e., $P_{\#}^{\theta}\mu_t * \mathcal{N}_{\sigma}$. The probabilistic counterpart to the evolution $(\mu_t)_{t \geq 0}$ in Equation (13) is a stochastic process $(X_t)_{t \geq 0}$ that solves for the following continuous-time stochastic differential equation (SDE) starting at $X_0 \sim \mu_0$:

$$dX_t = v^{(\sigma)}(X_t, \mu_t)dt + \sqrt{2\lambda}dW_t, \quad (16)$$

where $(W_t)_t$ is the Wiener process. As noted by Liutkus et al. (2019) for the case of regularized \mathcal{SW}_2 flow, the dependence of the drift $v^{(\sigma)}$ on X_t is reminiscent of McKean-Vlasov SDEs (Mishura & Veretennikov, 2020). The SDE (16) can be discretized using the Euler-Maruyama scheme with the initialization $\widehat{X}_0 \sim \mu_0$ as follows:

$$\widehat{X}_{k+1} = hv^{(\sigma)}(\widehat{X}_k, \widehat{\mu}_{kh}) + \sqrt{2\lambda h}Z_{k+1}, \quad (17)$$

where $h > 0$ is the step size, $\widehat{\mu}_{kh}$ is the distribution of \widehat{X}_k , and $\{Z_k\}_k$ are i.i.d. standard normal random variables.

The discrete-time SDE in (17) can then be simulated by a stochastic particle system $\{\widehat{X}_k^i\}$, where $i \in \{1, \dots, N\}$ is the index for the i^{th} particle, and the discrete time index k runs from 0 to $Kh = T$ (Bossy & Talay, 1997). The particles are initialized as $\widehat{X}_0^i \sim \mu_0$ i.i.d., where each particle follows the following update equation:

$$\widehat{X}_{k+1}^i = h\widehat{v}^{(\sigma)}(\widehat{X}_k^i) + \sqrt{2\lambda h}Z_{k+1}^i, \quad (18)$$

where $\widehat{v}^{(\sigma)}(\widehat{X}_k^i)$ is an estimate of $v^{(\sigma)}(\widehat{X}_k, \widehat{\mu}_{kh})$. To evaluate $\widehat{v}^{(\sigma)}$, we make two approximations.

1. The distribution $\widehat{\mu}_{kh}$ is approximated by the empirical distribution of the particles at time k .

$$\widehat{\mu}_{kh} \approx \widehat{\mu}_{kh}^{(N)} := \frac{1}{N} \sum_{i=1}^N \delta_{X_k^i}. \quad (19)$$

2. The integral over $\theta \in \mathbb{S}^{d-1}$ in $v^{(\sigma)}$ is approximated by a Monte Carlo estimate.

$$\widehat{v}_k(x) := -\frac{1}{N_{\theta}} \sum_{j=1}^{N_{\theta}} (\psi_{k,\theta_j}^{(\sigma)})'(\langle x, \theta_j \rangle) \theta_j, \quad (20)$$

where $(\psi_{k,\theta_j}^{(\sigma)})'$ is the derivative of the Kantorovich potential between $P_{\#}^{\theta_j} \widehat{\mu}_{kh}^{(N)} * \xi_{\sigma}$ and $P_{\#}^{\theta_j} \nu * \xi_{\sigma}$ with $\xi_{\sigma} \sim \mathcal{N}(0, \sigma^2)$. Using the closed-form expression for the optimal transport map in one-dimension stated in (6) and Brenier's theorem (Brenier, 1991), we can compute $(\psi_{k,\theta_j}^{(\sigma)})'$ as

$$(\psi_{k,\theta_j}^{(\sigma)})'(z) = z - F_{P_{\#}^{\theta_j} \widehat{\mu}_{kh}^{(N)} * \xi_{\sigma}}^{-1} \circ F_{P_{\#}^{\theta_j} \nu * \xi_{\sigma}}(z). \quad (21)$$

Algorithm 1: Differentially Private Sliced Wasserstein Flow with resampling of θ 's: DPSWflow-r.

Input: $Y = [Y_1^T, \dots, Y_n^T]^T \in \mathbb{R}^{n \times d}$ i.e. N i.i.d. samples from target distribution ν , number of projections N_{θ} , regularization parameter λ , variance σ , step size h .

Output: $\{\widehat{X}_i\}_{i=1}^N$

```

// Initialize the particles
1  $\{\widehat{X}_0^i\}_{i=1}^N \sim \mu_0, \widehat{X} = [x_1^T, \dots, x_n^T]^T \in \mathbb{R}^{n \times d};$ 
// Iterations
2 for  $k = 0, \dots, K - 1$  do
3    $\{\theta_j\}_{j=1}^{N_{\theta}} \sim \text{Unif}(\mathbb{S}^{d-1}), \Theta = [\theta_1^T, \dots, \theta_{N_{\theta}}^T];$ 
4   Sample  $Z_X, Z_Y \in \mathbb{R}^{n \times N_{\theta}}$  from i.i.d  $\mathcal{N}(0, \sigma^2);$ 
5   Compute the quantiles of  $Y\Theta + Z_Y;$ 
6   Compute the CDF of  $X\Theta + Z_X;$ 
7   Compute  $\widehat{v}^{(\sigma)}(\widehat{X}_k^i)$  using (20) and (21);
8    $\widehat{X}_{k+1}^i \leftarrow h\widehat{v}^{(\sigma)}(\widehat{X}_k^i) + \sqrt{2\lambda h}Z,$  where  $Z \sim \mathcal{N}(0, \mathcal{I}_d).$ 

```

Note that the target distribution ν is approximated by the empirical distribution of samples from the dataset in practice.

In the infinite particle regime, i.e., as $N \rightarrow \infty$, under some assumptions of regularity and smoothness of the drift terms $v^{(\sigma)}$ and $\widehat{v}^{(\sigma)}$, the following theorem bounds the error in approximating the continuous time SDE in Equation (16) by the discrete-time update equation in Equation (18).

Theorem 2. *Suppose that the SDE in (16) has a unique strong solution $(X_t)_{t \in [0, T]}$ for any starting point $x_0 \in \Omega$ such that $X_T \sim \mu_T$. For $T = Kh$, let $\widehat{\mu}_{Kh}$ be the distribution of \widehat{X}_K in the discrete-time SDE in Equation (17). Under suitable assumptions of regularity and Lipschitzness on $v^{(\sigma)}$ and $\widehat{v}^{(\sigma)}$ stated in the supplementary document, the following bound holds for any $\lambda > TL_{\sigma}^2/8$:*

$$\|\mu_T - \widehat{\mu}_{Kh}\|_{TV}^2 \leq \frac{T}{\lambda - TL_{\sigma}^2/8} \left[L_{\sigma}^2 h (c_1 h + d\lambda) + c_2 \delta \right], \quad (22)$$

where $C_1, c_2, L_{\sigma}, \delta > 0$ are constants independent of time.

The above theorem follows in a straightforward manner from a similar theorem of Liutkus et al. (2019) for the \mathcal{SW}_2 flow.

4.3 Privacy Guarantee

In this subsection we analyze the DP guarantee of the particle scheme outlined in the previous subsection. In

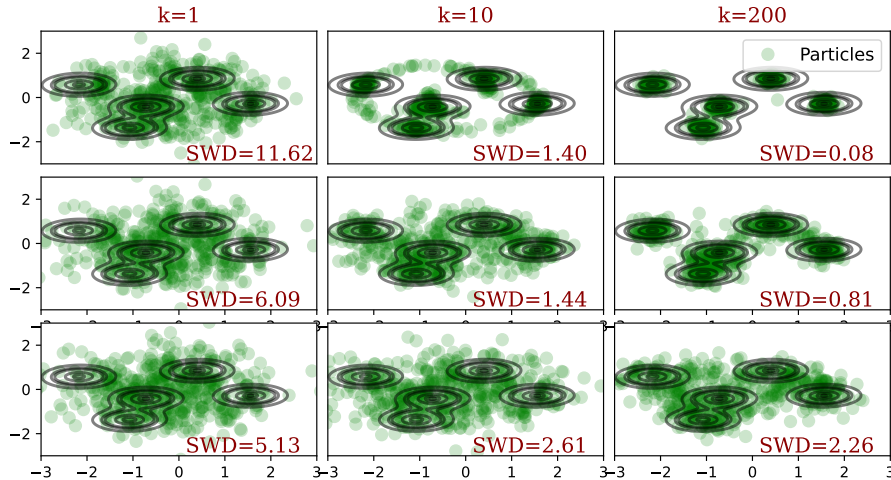


Figure 1: Examples of particle flows for (top) sliced Wasserstein flow, (middle) our DPSWflow with $\sigma = 0.5$, and (bottom) $\sigma = 1$. Each panel shows the level sets (in black) of the target distribution, which is composed of 5 Gaussians, as well as the particles (in green). The columns depict the particles after the (left) first step, (middle) 10-th, and (right) the 200-th steps of the flow.

each iteration of the particle system, the drift terms of the particles in the update equation are computed using (20) and (21). Crucially, samples from the true data distribution are only used in a single step - the computation of $(\psi_{k,\theta_j}^{(\sigma)})'$ along each projection θ_j on the unit sphere via (21). Let $\Theta = [\theta_1^T, \dots, \theta_{N_\theta}^T] \in \mathbb{R}^{d \times N_\theta}$ denote the *random projection matrix* composed of all the N_θ projection vectors sampled uniformly from \mathbb{S}^{d-1} . Let $X = [x_1^T, \dots, x_n^T]^T \in \mathbb{R}^{n \times d}$ denote the *data matrix* composed of the n i.i.d. samples from the target distribution ν . We define a randomized mechanism $\mathcal{M}_{N_\theta, \sigma}: \mathbb{R}^{n \times d} \rightarrow \mathbb{R}^{n \times N_\theta}$ as

$$\mathcal{M}_{N_\theta, \sigma}(X) = X\Theta + Z, \quad (23)$$

where Θ is the random projection matrix and $Z \in \mathbb{R}^{n \times N_\theta}$ consists of i.i.d. Gaussian random variables with variance σ^2 . Given X composed of $\{x_i\}_i \sim \nu$, the position of the particles can be updated through Equations (20) and (21) simply by having access to $\mathcal{M}_{N_\theta, \sigma}(X)$. Hence, if $\mathcal{M}_{N_\theta, \sigma}(X)$ is (ϵ, δ) -DP, then by the post-processing property of DP, the particle system update is also (ϵ, δ) -DP. The following lemma from Rakotomamonjy & Ralaivola (2021) gives the DP guarantee for $\mathcal{M}_{N_\theta, \sigma}(X)$.

Lemma 1 (Rakotomamonjy & Ralaivola (2021)). For data matrices $X, X' \in \mathbb{R}^{n \times d}$ that differ in only the i^{th} row, satisfying $\|X_i - X'_i\|_2 \leq 1$ and a random projection matrix $\Theta \in \mathbb{R}^{d \times N_\theta}$ whose columns are randomly sampled from \mathbb{S}^{d-1} , the following bound holds with probability at least $1 - \delta$:

$$\|X\Theta - X'\Theta\|_F^2 \leq w(N_\theta, \delta), \quad (24)$$

with

$$w(N_\theta, \delta) = \frac{N_\theta}{d} + \frac{2}{3} \ln \frac{2}{\delta} + \frac{2}{d} \sqrt{N_\theta \frac{d-1}{d+2} \ln \frac{2}{\delta}}. \quad (25)$$

By using the Central Limit Theorem (CLT) and assuming that k is large enough ($k > 30$), we get under the same hypotheses that the following holds:

$$w(N_\theta, \delta) = \frac{N_\theta}{d} + \frac{z_{1-\delta}}{d} \sqrt{\frac{2N_\theta(d-1)}{d+2}}, \quad (26)$$

where $z_{1-\delta} = \Phi^{-1}(1-\delta)$ and Φ is the cumulative distribution function of a zero-mean unit variance Gaussian distribution.

In practice we use Equation 26 to compute the bound on the sensitivity.

Plugging in the sensitivity bound from Lemma 1 into the Gaussian mechanism presented in Section 2.1, we see that the mechanism $\mathcal{M}_{N_\theta, \sigma}$ is (ϵ, δ) -DP for:

$$\sigma \geq \frac{cw(N_\theta, \delta)}{\epsilon}, \quad (27)$$

for some constant $c > 2 \ln(1.25/\delta)$. We observe that the privacy parameter ϵ degrades linearly with the number of projections N_θ .

5 EXPERIMENTS

In this section we evaluate our method within a generative modeling context. The primary objective is to validate our theoretical framework and showcase

the behavior of our approach, rather than striving for state-of-the-art results in generative modeling.

To maintain a suitably low input space dimension, in order to mitigate the curse of dimensionality and ensure lower computational cost, our Algorithm 1 is preceded by an autoencoder with $\mathcal{Z}_{\mu,\sigma}$ as the latent space. Subsequently, Algorithm 1 takes the Gaussian composed latent space $\mathcal{Z}_\mu \subseteq \mathbb{R}^d$ of the autoencoder as the input space, and ensures differential privacy using the DP gradient flow approach that we have previously described in Section 4.2.

5.1 Comparisons and Baselines

With the objective of evaluating our main method DPSWflow-r (Algorithm 1), we implement and present two variants of our approach: the former is DPSWflow (Algorithm 2), a variant of DPSWflow-r that omits resampling of the projections θ at each step of the flow. Instead, we generate N_θ random directions $\theta_n \sim \text{Uniform}(\mathbb{S}^{d-1})$ and store them in the vector Θ . During each iteration of the flow, we sample M_θ random directions from Θ where $M_\theta < N_\theta$. The latter variant is DPSWgen from Rakotomamonjy & Ralaivola (2021), which is a generator-based model (different than a flow). DPSWgen employs DP SW as loss for training generator, while our contribution is to build a gradient flow that is DP because its drift term is approximated by the DP SW. Both approaches are fundamentally distinct. We use this baseline to show that our DPSWflow-r method outperforms generator-based methods trained with the same DP metric.

To ensure a fair comparison, the DPSWgen generator is built with the same architecture as the decoder of DPSWflow-r and DPSWflow. We evaluate the three methods using the Fréchet inception distance (FID) (Heusel et al., 2018). In our results, we present each method at three levels of differential privacy: $\epsilon = \infty$ (no privacy), $\epsilon = 10$, and $\epsilon = 5$, along with their corresponding FID scores.

We also evaluate each model with and without the application of differential privacy, using the non-private model as a point of reference. In this context, the optimal generated images from each model are expected to yield the best achievable FID score when $\epsilon = \infty$.

5.2 Sensitivity and Privacy Budget Tracking

For both DPSWflow-r and DPSWgen, we monitor the privacy budget using the Gaussian moments accountant method proposed by Abadi et al. (2016), where we choose a range of σ 's satisfying the constraint in Equation (27) and use the moment accountant to obtain the corresponding ϵ 's.

Also, to prevent privacy leakage, we normalize the input of the flow to norm 1, so we incur an additional factor of 2 in the bound.

5.3 Datasets and Settings

In both the DPSWflow and DPSWflow-r models we pre-train an autoencoder and then use a DP sliced Wasserstein flow component. In order to uphold the integrity of the differential privacy framework and mitigate potential privacy breaches, we conducted separate pre-training procedures for the autoencoder and the DPSW-flow models using distinct datasets: a publicly available dataset for the autoencoder, and a confidential dataset for the flow model. In practice, we partitioned the training set X into two distinct segments of equal size, denoted as X^{pub} and X^{priv} . Subsequently, we conducted training of the autoencoder on X^{pub} . Then, we compute the encoded representation on X^{priv} in the latent space and use it as input to the DPSW-flow. To ensure fair comparison of the generated outcomes, we specifically trained the DPSWgen model on X^{priv} . Furthermore, as mentioned in Section 5.2, to prevent privacy leakage, we normalize the latent space before adding Gaussian noise, ensuring that the encoded representations lie on a hypersphere.

We assessed each method using two datasets: MNIST (LeCun et al., 1998) and FashionMNIST (Xiao et al., 2017). The experiments performed on the MNIST and FashionMNIST datasets use an autoencoder/generator architecture as per the framework proposed by Liutkus et al. (2019).

5.4 Toy Problem

We use a toy problem to illustrate how our differentially private sliced Wasserstein gradient flow behaves compared to the vanilla non-DP baseline. Here, we have set $N_\theta = 200$, $h = 1$, and $\lambda = 0.001$. Examples are provided in Figure 1. We see that the particle flow of the sliced Wasserstein can correctly approximate the target distributions that is composed of 5 Gaussians, as measured by SWD. With the Gaussian smoothing, for $\sigma = 0.5$, the particles are still able to match the target distribution, although samples are more dispersed than for the noiseless SWF, leading to a SWD value of 0.81 instead of 0.08. Finally, for $\sigma = 1$, our approach struggles in matching the true distribution, although many particles are still within the level sets of it.

5.5 Experimental Results

This section outlines our experimental findings. The resulting FID scores are shown in Table 1, and are calculated as the average of the FID scores obtained

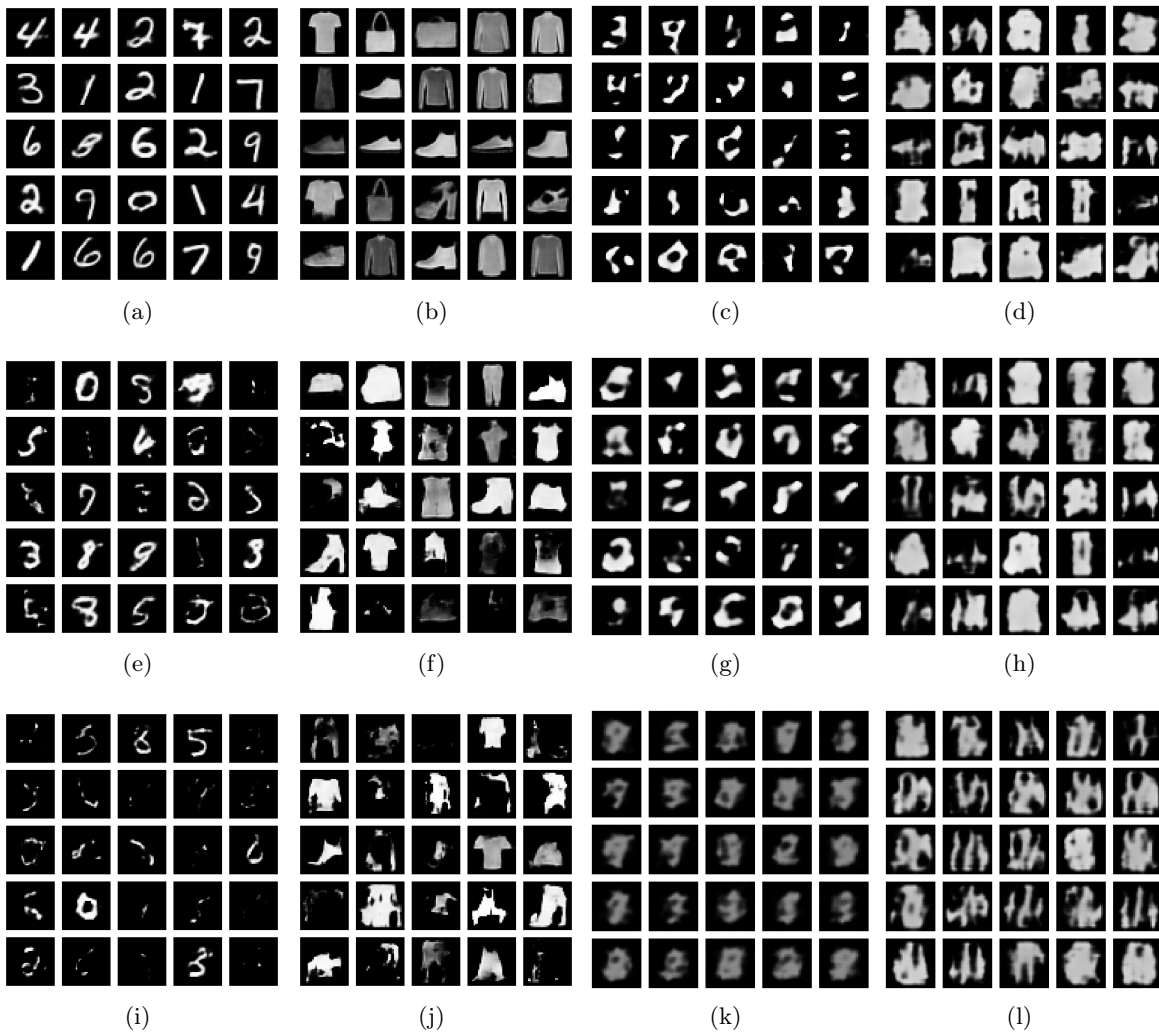


Figure 2: Examples of images generated with our method: DPSWflow-r (left: (a),(b),(e),(f),(i),(j)) and the baseline DPSWgen (right: (c),(d),(g),(h),(k),(l)). Each row shows a different level of DP: the first row is no DP ($\epsilon = \infty$), the second row is $\epsilon = 10$, and the third row is $\epsilon = 5$.

Table 1: Summary of the FID results for the main experiments we conducted.

	MNIST			F-MNIST			
	ϵ	∞	10	5	∞	10	5
DPSWgen		104	149	199	155	182	201
DPSWflow-r		21	71	117	42	88	99
DPSWflow		73	118	171	96	98	129

from five generation runs. Figure 2 shows samples collected from each of our experiments.

We observe that our methods outperform the DPSWgen baseline for all privacy budgets tested in our experiments, both in terms of FID scores and the visual quality of the generated samples. Furthermore, the variant of our approach with resampling (DPSWflow-r) consistently outperforms the variant without resampling (DPSWflow). These experiments show that our approach is practically viable and can serve as a promising basis for future work on private generative models.

More experiments are presented in Appendix D.

6 CONCLUSION

In this paper we have introduced a novel theoretically grounded approach for differentially private generative modeling. Our approach leverages gradient flows within the Wasserstein space, with a drift term computed using the differentially private sliced Wasserstein distance. To the best of our knowledge, we are the first to propose such a DP gradient flow approach. Our experiments have shown that our approach is practically viable. With both a strong theoretical foundation and experimental viability, we believe that our method forms a promising basis for future work in the area of private generative modeling.

References

- Abadi, M., Chu, A., Goodfellow, I., McMahan, H. B., Mironov, I., Talwar, K., and Zhang, L. Deep learning with differential privacy. In *Proceedings of the 2016 ACM SIGSAC Conference on Computer and Communications Security*. ACM, oct 2016. doi: 10.1145/2976749.2978318. URL <https://doi.org/10.1145/2976749.2978318>.
- Aggarwal, R., Sounderajah, V., Martin, G., Ting, D. S., Karthikesalingam, A., King, D., Ashrafian, H., and Darzi, A. Diagnostic accuracy of deep learning in medical imaging: a systematic review and meta-analysis. *NPJ digital medicine*, 4(1):65, 2021.
- Ambrosio, L. Gradient flows in metric spaces and in the spaces of probability measures, and applications to fokker-planck equations with respect to log-concave measures. *Bollettino dell’Unione Matematica Italiana*, 1(1):223–240, 2 2008. URL <http://eudml.org/doc/290477>.
- Arjovsky, M., Chintala, S., and Bottou, L. Wasserstein GAN. In *Proceedings of the 34th International Conference on Machine Learning, Sydney, Australia*, December 2017. URL <http://arxiv.org/abs/1701.07875>. arXiv: 1701.07875.
- Benamou, J.-D. and Brenier, Y. A computational fluid mechanics solution to the monge-kantorovich mass transfer problem. *Numerische Mathematik*, 84(3): 375–393, 2000.
- Bonet, C., Courty, N., Septier, F., and Drumetz, L. Efficient gradient flows in sliced-wasserstein space. *Transactions on Machine Learning Research*, 2022. ISSN 2835-8856. URL <https://openreview.net/forum?id=Au1LNKmRvh>.
- Bonnotte, N. *Unidimensional and evolution methods for optimal transportation*. PhD thesis, Université Paris Sud-Paris XI; Scuola normale superiore (Pise, Italie), 2013.
- Bossy, M. and Talay, D. A stochastic particle method for the mckean-vlasov and the burgers equation. *Mathematics of computation*, 66(217):157–192, 1997.
- Bousquet, O., Gelly, S., Tolstikhin, I., Simon-Gabriel, C.-J., and Schoelkopf, B. From optimal transport to generative modeling: the vegan cookbook. *arXiv preprint arXiv:1705.07642*, 2017.
- Brenier, Y. Polar factorization and monotone rearrangement of vector-valued functions. *Communications on pure and applied mathematics*, 44(4):375–417, 1991.
- Brenier, Y., Frisch, U., Hénon, M., Loeper, G., Matarrese, S., Mohayaee, R., and Sobolevskii, A. Reconstruction of the early universe as a convex optimization problem. *Monthly Notices of the Royal Astronomical Society*, 346(2):501–524, 2003.
- Cao, T., Bie, A., Vahdat, A., Fidler, S., and Kreis, K. Don’t generate me: Training differentially private generative models with sinkhorn divergence. *Advances in Neural Information Processing Systems*, 34:12480–12492, 2021.
- Carlini, N., Hayes, J., Nasr, M., Jagielski, M., Sehwag, V., Tramèr, F., Balle, B., Ippolito, D., and Wallace, E. Extracting training data from diffusion models. In *32nd USENIX Security Symposium (USENIX Security 23)*, pp. 5253–5270, Anaheim, CA, August 2023. USENIX Association. ISBN 978-1-939133-37-3. URL <https://www.usenix.org/conference/usenixsecurity23/presentation/carlini>.
- Chen, D., Orekondy, T., and Fritz, M. Gs-wgan: A gradient-sanitized approach for learning differentially private generators. In Larochelle, H., Ranzato, M., Hadsell, R., Balcan, M., and Lin, H. (eds.), *Advances in Neural Information Processing Systems*, volume 33, pp. 12673–12684. Curran Associates, Inc., 2020a. URL https://proceedings.neurips.cc/paper_files/paper/2020/file/9547ad6b651e2087bac67651aa92cd0d-Paper.pdf.
- Chen, D., Yu, N., Zhang, Y., and Fritz, M. Ganleaks: A taxonomy of membership inference attacks against generative models. In *Proceedings of the 2020 ACM SIGSAC conference on computer and communications security*, pp. 343–362, 2020b.
- Cullen, M. J. P. *A mathematical theory of large-scale atmosphere/ocean flow*. World Scientific, 2006.
- Dockhorn, T., Cao, T., Vahdat, A., and Kreis, K. Differentially private diffusion models. *Transactions on Machine Learning Research*, 2023. ISSN 2835-8856. URL <https://openreview.net/forum?id=ZPpQk7FJXF>.
- Dwork, C. A firm foundation for private data analysis. *Commun. ACM*, 54:86–95, 04 2011. doi: 10.1145/1866739.1866758.

- Dwork, C. and Roth, A. The algorithmic foundations of differential privacy. *Found. Trends Theor. Comput. Sci.*, 9(3–4):211–407, aug 2014. ISSN 1551-305X. doi: 10.1561/0400000042. URL <https://doi.org/10.1561/0400000042>.
- Dwork, C., McSherry, F., Nissim, K., and Smith, A. Calibrating noise to sensitivity in private data analysis. In *Theory of Cryptography Conference*, volume Vol. 3876, pp. 265–284, 01 2006. ISBN 978-3-540-32731-8. doi: 10.1007/11681878_14.
- Genevay, A., Peyré, G., and Cuturi, M. Gan and vae from an optimal transport point of view. *arXiv preprint arXiv:1706.01807*, 2017.
- Genevay, A., Peyré, G., and Cuturi, M. Learning generative models with sinkhorn divergences. In *International Conference on Artificial Intelligence and Statistics*, pp. 1608–1617. PMLR, 2018.
- Ghalebikesabi, S., Berrada, L., Goyal, S., Ktena, I., Stanforth, R., Hayes, J., De, S., Smith, S. L., Wiles, O., and Balle, B. Differentially private diffusion models generate useful synthetic images. *arXiv preprint arXiv:2302.13861*, 2023.
- Harder, F., Adamczewski, K., and Park, M. DP-MERF: Differentially private mean embeddings with random features for practical privacy-preserving data generation. In Banerjee, A. and Fukumizu, K. (eds.), *Proceedings of The 24th International Conference on Artificial Intelligence and Statistics*, volume 130 of *Proceedings of Machine Learning Research*, pp. 1819–1827. PMLR, 13–15 Apr 2021. URL <https://proceedings.mlr.press/v130/harder21a.html>.
- Harder, F., Jalali, M., Sutherland, D. J., and Park, M. Pre-trained perceptual features improve differentially private image generation. *Transactions on Machine Learning Research*, 2023. ISSN 2835-8856. URL <https://openreview.net/forum?id=R6W7zkMzOP>.
- Heusel, M., Ramsauer, H., Unterthiner, T., Nessler, B., and Hochreiter, S. Gans trained by a two time-scale update rule converge to a local nash equilibrium, 2018.
- Hu, H., Salcic, Z., Sun, L., Dobbie, G., Yu, P. S., and Zhang, X. Membership inference attacks on machine learning: A survey, 2022.
- Jordan, R., Kinderlehrer, D., and Otto, F. The variational formulation of the Fokker-Planck equation. 1 1996. doi: 10.1184/R1/6480020.v1. URL https://kithub.cmu.edu/articles/journal_contribution/The_variational_formulation_of_the_Fokker-Planck_equation/6480020.
- Lacharité, M.-S., Minaud, B., and Paterson, K. G. Improved reconstruction attacks on encrypted data using range query leakage. In *2018 IEEE Symposium on Security and Privacy (SP)*, pp. 297–314. IEEE, 2018.
- Lê Tien, N., Habrard, A., and Sebban, M. Differentially private optimal transport: Application to domain adaptation. In *IJCAI*, pp. 2852–2858, 2019.
- LeCun, Y., Bottou, L., Bengio, Y., and Haffner, P. Gradient-based learning applied to document recognition. *Proceedings of the IEEE*, 86(11):2278–2324, November 1998.
- Liu, Z., Luo, P., Wang, X., and Tang, X. Deep learning face attributes in the wild. In *Proceedings of International Conference on Computer Vision (ICCV)*, December 2015.
- Liutkus, A., Simsekli, U., Majewski, S., Durmus, A., and Stöter, F.-R. Sliced-wasserstein flows: Nonparametric generative modeling via optimal transport and diffusions. In *International Conference on Machine Learning*, pp. 4104–4113. PMLR, 2019.
- Long, Y., Wang, B., Yang, Z., Kailkhura, B., Zhang, A., Gunter, C., and Li, B. G-pate: Scalable differentially private data generator via private aggregation of teacher discriminators. In Ranzato, M., Beygelzimer, A., Dauphin, Y., Liang, P., and Vaughan, J. W. (eds.), *Advances in Neural Information Processing Systems*, volume 34, pp. 2965–2977. Curran Associates, Inc., 2021. URL https://proceedings.neurips.cc/paper_files/paper/2021/file/171ae1bbb81475eb96287dd78565b38b-Paper.pdf.
- Mai, G., Cao, K., Yuen, P. C., and Jain, A. K. On the reconstruction of face images from deep face templates. *IEEE transactions on pattern analysis and machine intelligence*, 41(5):1188–1202, 2018.
- Mishura, Y. and Veretennikov, A. Existence and uniqueness theorems for solutions of mckean–vlasov stochastic equations. *Theory of Probability and Mathematical Statistics*, 103:59–101, 2020.
- Radford, A., Metz, L., and Chintala, S. Unsupervised representation learning with deep convolutional generative adversarial networks. In *International Conference on Learning Representations*, 2016.
- Rakotomamonjy, A. and Ralaivola, L. Differentially private sliced wasserstein distance, 2021.
- Rakotomamonjy, A., Alaya, M. Z., Berar, M., and Gasso, G. Statistical and topological properties of gaussian smoothed sliced probability divergences. *arXiv preprint arXiv:2110.10524*, 2021.
- Salimans, T., Goodfellow, I., Zaremba, W., Cheung, V., Radford, A., and Chen, X. Improved Techniques for Training GANs, June 2016. URL <http://arxiv.org/abs/1606.03498>. arXiv:1606.03498 [cs].
- Santambrogio, F. Euclidean, Metric, and Wasserstein gradient flows: an overview, 2016.

-
- Shen, D., Wu, G., and Suk, H.-I. Deep learning in medical image analysis. *Annual review of biomedical engineering*, 19:221–248, 2017.
- Shokri, R., Stronati, M., Song, C., and Shmatikov, V. Membership inference attacks against machine learning models. In *2017 IEEE Symposium on Security and Privacy (SP)*, pp. 3–18, 2017.
- Xiao, H., Rasul, K., and Vollgraf, R. Fashion-mnist: a novel image dataset for benchmarking machine learning algorithms, 2017.
- Xie, L., Lin, K., Wang, S., Wang, F., and Zhou, J. Differentially private generative adversarial network. *arXiv preprint arXiv:1802.06739*, 2018.

A PROOF of THEOREM 1

We begin by presenting two propositions that generalize Proposition 5.1.6 and Proposition 5.1.7 of [Bonnotte \(2013\)](#), respectively. These propositions will play a crucial role in the proof of Theorem 1, and constitute a key element of novelty in our proof, compared to the proof of Theorem 2 in [Liutkus et al. \(2019\)](#).

Indeed, the $\mathcal{G}_\sigma \mathcal{SW}_2^2$ metric is not a simple application of the sliced Wasserstein metric to Gaussian convoluted measures. The convolution with Gaussian measure in the $\mathcal{G}_\sigma \mathcal{SW}_2^2$ metric occurs within the surface integral, separately for each one-dimensional projection of the original measures. This distinction becomes clear when comparing equations 7 with 11. Hence, establishing a DP gradient flow presented a unique challenge which makes a distinct contribution. The distinct nature of $\mathcal{G}_\sigma \mathcal{SW}_2^2$ metric introduces two blockers that need to be circumvented before applying results from [Bonnotte \(2013\)](#) and [Liutkus et al. \(2019\)](#), namely the existence and regularity of minimizers to the functional in Equation 12. Both these steps are non-trivial.

Proposition 1. Let $\mu, \nu \in \mathcal{P}(\Omega)$. For any $\bar{\mu} \in \mathcal{P}(\Omega)$,

$$\lim_{\varepsilon \rightarrow 0^+} \frac{\mathcal{G}_\sigma \mathcal{SW}_2^2((1-\varepsilon)\mu + \varepsilon\bar{\mu}, \nu) - \mathcal{G}_\sigma \mathcal{SW}_2^2(\mu, \nu)}{2\varepsilon} = \int_{\mathbb{S}^{d-1}} \int_{\Omega} \psi_{\theta, \sigma}(\langle \theta, x \rangle) d(\bar{\mu} - \mu) d\theta, \quad (28)$$

where $\psi_{\theta, \sigma}$ is a Kantorovich potential between $\theta_{\sharp} \mu * \mathcal{N}_\sigma$ and $\theta_{\sharp} \nu * \mathcal{N}_\sigma$.

Proof. Since $\theta_{\sharp} \nu * \mathcal{N}_\sigma$ is absolutely continuous with respect to the Lebesgue measure for any $\theta \in \mathbb{S}^{d-1}$, there indeed exists a Kantorovich potential $\psi_{\theta, \sigma}$ between $\theta_{\sharp} \mu * \mathcal{N}_\sigma$ and $\theta_{\sharp} \nu * \mathcal{N}_\sigma$. Since $\psi_{\theta, \sigma}$ may not be optimal between $(1-\varepsilon)\mu + \varepsilon\bar{\mu}$ and ν ,

$$\liminf_{\varepsilon \rightarrow 0^+} \frac{\mathcal{G}_\sigma \mathcal{SW}_2^2((1-\varepsilon)\mu + \varepsilon\bar{\mu}, \nu) - \mathcal{G}_\sigma \mathcal{SW}_2^2(\mu, \nu)}{2\varepsilon} \geq \int \int \psi_{\theta, \sigma}(\langle \theta, x \rangle) d(\bar{\mu} - \mu) d\theta. \quad (29)$$

Conversely, let $\psi_{\theta, \sigma}^\varepsilon$ be a Kantorovich potential between $\theta_{\sharp}[(1-\varepsilon)\mu + \varepsilon\bar{\mu}] * \mathcal{N}_\sigma$ and $\theta_{\sharp} \nu * \mathcal{N}_\sigma$ with $\int \psi_{\theta, \sigma}^\varepsilon d\theta_{\sharp}[(1-\varepsilon)\mu + \varepsilon\bar{\mu}] * \mathcal{N}_\sigma$. Then,

$$\frac{1}{2} \mathcal{G}_\sigma \mathcal{SW}_2^2((1-\varepsilon)\mu + \varepsilon\bar{\mu}, \nu) - \frac{1}{2} \mathcal{G}_\sigma \mathcal{SW}_2^2(\mu, \nu) \leq \varepsilon \int \int \psi_{\theta, \sigma}^\varepsilon(\langle \theta, x \rangle) d(\bar{\mu} - \mu) d\theta. \quad (30)$$

As in the proof of Proposition 5.1.6 in [Bonnotte \(2013\)](#), $\psi_{\theta, \sigma}^\varepsilon$ uniformly converges to a Kantorovich potential for $(\theta_{\sharp} \mu * \mathcal{N}_\sigma, \theta_{\sharp} \nu * \mathcal{N}_\sigma)$ as $\varepsilon \rightarrow 0^+$. Hence,

$$\limsup_{\varepsilon \rightarrow 0^+} \frac{\mathcal{G}_\sigma \mathcal{SW}_2^2((1-\varepsilon)\mu + \varepsilon\bar{\mu}, \nu) - \mathcal{G}_\sigma \mathcal{SW}_2^2(\mu, \nu)}{2\varepsilon} \leq \int \int \psi_{\theta, \sigma}^\varepsilon(\langle \theta, x \rangle) d(\bar{\mu} - \mu) d\theta. \quad (31)$$

Combining (30) and (31), we get the desired result. \square

Proposition 2. Let $\mu, \nu \in \mathcal{P}(\Omega)$. For any diffeomorphism ζ of Ω ,

$$\lim_{\varepsilon \rightarrow 0^+} \frac{\mathcal{G}_\sigma \mathcal{SW}_2^2([\text{Id} + \varepsilon\zeta]_{\sharp} \mu, \nu) - \mathcal{G}_\sigma \mathcal{SW}_2^2(\mu, \nu)}{2\varepsilon} = \int_{\mathbb{S}^{d-1}} \int_{\Omega} \psi'_{\theta, \sigma}(\langle \theta, x \rangle) \langle \theta, \zeta(x) \rangle d\mu d\theta, \quad (32)$$

where $\psi_{\theta, \sigma}$ is a Kantorovich potential between $\theta_{\sharp} \mu * \mathcal{N}_\sigma$ and $\theta_{\sharp} \nu * \mathcal{N}_\sigma$.

Proof. Using the fact that $\psi_{\theta, \sigma}$ is a Kantorovich potential between $\theta_{\sharp} \mu * \mathcal{N}_\sigma$ and $\theta_{\sharp} \nu * \mathcal{N}_\sigma$, we get the following:

$$\frac{\mathcal{G}_\sigma \mathcal{SW}_2^2([\text{Id} + \varepsilon\zeta]_{\sharp} \mu, \nu) - \mathcal{G}_\sigma \mathcal{SW}_2^2(\mu, \nu)}{2\varepsilon} \geq \int_{\mathbb{S}^{d-1}} \int_{\Omega} \frac{\psi_{\theta, \sigma}(\langle \theta, x + \varepsilon\zeta(x) \rangle) - \psi_{\theta, \sigma}(\langle \theta, x \rangle)}{2\varepsilon} d\mu d\theta. \quad (33)$$

Since the Kantorovich potential is Lipschitz, it is differentiable almost everywhere, and so, we get the following using Lebesgue's differentiation theorem:

$$\liminf_{\varepsilon \rightarrow 0^+} \frac{\mathcal{G}_\sigma \mathcal{SW}_2^2([\text{Id} + \varepsilon\zeta]_{\sharp} \mu, \nu) - \mathcal{G}_\sigma \mathcal{SW}_2^2(\mu, \nu)}{2\varepsilon} \geq \int_{\mathbb{S}^{d-1}} \int_{\Omega} \psi'_{\theta, \sigma}(\langle \theta, x \rangle) \langle \theta, \zeta(x) \rangle d\mu d\theta. \quad (34)$$

Conversely, we will now show the same upper bound on the lim sup. Let $\gamma_{\theta,\sigma} \in \Pi(\theta_{\#}\mu * \mathcal{N}_{\sigma}, \theta_{\#}\nu * \mathcal{N}_{\sigma})$ be the optimal transport plan corresponding to $\psi_{\theta,\sigma}$. As is done in Proposition 5.1.7 in [Bonnotte \(2013\)](#), we extend $\gamma_{\theta,\sigma}$ to $\pi_{\theta,\sigma} \in \Pi(\mu, \nu)$ such that $(\theta \otimes \theta)_{\#}\pi_{\theta,\sigma} = \gamma_{\theta,\sigma}$. In other words, if random variables (X, Y) are sampled from $\pi_{\theta,\sigma}$, then $(\langle X, \theta \rangle, \langle Y, \theta \rangle)$ will follow the law of $\gamma_{\theta,\sigma}$ for every $\theta \in \mathbb{S}^{d-1}$. Then, it follows that $[\theta + \varepsilon\zeta(\zeta) \otimes \theta]_{\#}\pi_{\theta} \in \Pi(\theta_{\#}[\text{Id} + \varepsilon\zeta]_{\#}\mu, \theta_{\#}\nu)$. Hence,

$$\mathcal{G}_{\sigma}\mathcal{SW}_2^2([\text{Id} + \varepsilon\zeta]_{\#}\mu, \nu) - \mathcal{G}_{\sigma}\mathcal{SW}_2^2(\mu, \nu) \leq \int \int |\langle \theta, x + \varepsilon\zeta(x) - y \rangle|^2 - |\langle \theta, x - y \rangle|^2 d\pi_{\theta,\sigma}(x, y) d\theta.$$

Since $\pi_{\theta,\sigma}$ is constructed from $\gamma_{\theta,\sigma}$, which in turn is based on the Kantorovich potential $\psi_{\theta,\sigma}$, we have $\langle \theta, y \rangle = \langle \theta, x \rangle - \psi'_{\theta,\sigma}(\langle \theta, x \rangle)$ for $\pi_{\theta,\sigma}$ -a.e. (x, y) , because of the optimality of $\gamma_{\theta,\sigma}$ for the one-dimensional optimal transport. Therefore,

$$\mathcal{G}_{\sigma}\mathcal{SW}_2^2([\text{Id} + \varepsilon\zeta]_{\#}\mu, \nu) - \mathcal{G}_{\sigma}\mathcal{SW}_2^2(\mu, \nu) \leq \int \int |\psi'_{\theta,\sigma}(\langle \theta, x \rangle) - \varepsilon\langle \theta, \zeta(x) \rangle|^2 - |\psi'_{\theta,\sigma}(\langle \theta, x \rangle)|^2 d\pi_{\theta,\sigma}(x, y) d\theta.$$

Simplifying the right hand side of the above equation and taking the limit of $\varepsilon \rightarrow 0^+$, we get the following:

$$\limsup_{\varepsilon \rightarrow 0^+} \frac{\mathcal{G}_{\sigma}\mathcal{SW}_2^2([\text{Id} + \varepsilon\zeta]_{\#}\mu, \nu) - \mathcal{G}_{\sigma}\mathcal{SW}_2^2(\mu, \nu)}{2\varepsilon} \leq \int_{\mathbb{S}^{d-1}} \int_{\Omega} \psi'_{\theta,\sigma}(\langle \theta, x \rangle) \langle \theta, \zeta(x) \rangle d\mu d\theta. \quad (35)$$

Combining (35) and (34), we get the desired result. \square

We reproduce the following definition from [\(Liutkus et al., 2019\)](#).

Definition 2. (Generalized Minimizing Movement Scheme (GMMS)) Let $r > 0$ and $\mathcal{F} : \mathbb{R}_+ \times \mathcal{P}(\overline{\mathbb{B}}(0, r)) \times \mathcal{P}(\overline{\mathbb{B}}(0, r)) \rightarrow \mathbb{R}$ be a functional. For $h > 0$, let $\mu^h : [0, \infty) \rightarrow \mathcal{P}(\overline{\mathbb{B}}(0, r))$ be a piecewise constant trajectory for \mathcal{F} starting at $\mu_0 \in \mathcal{P}(\overline{\mathbb{B}}(0, r))$, such that: (i) $\mu^h(0) = \mu_0$, (ii) $\mu^h(t) = \mu^h(nh)$ for $n = \lfloor t/h \rfloor$, and (iii) $\mu^h((n+1)h)$ minimizes the functional $\zeta \mapsto \mathcal{F}(h, \zeta, \mu^h(nh))$, for all $n \in \mathbb{N}$.

We say that $\hat{\mu}$ is a Minimizing Movement Scheme (MMS) for \mathcal{F} starting at μ_0 if there exists a family of piecewise constant trajectories $(\mu^h)_{h>0}$ for \mathcal{F} such that $\lim_{h \rightarrow 0} \mu^h(t) = \hat{\mu}(t)$ for all $t \in \mathbb{R}_+$.

We say that $\tilde{\mu}$ is a Generalized Minimizing Movement Scheme (GMMS) for \mathcal{F} starting at μ_0 if there exists a family of piecewise constant trajectories $(\mu^{h_n})_{n \in \mathbb{N}}$ for \mathcal{F} such that $\lim_{n \rightarrow \infty} \mu^{h_n}(t) = \tilde{\mu}(t)$ for all $t \in \mathbb{R}_+$.

Theorem 3 (Existence of solution to the minimization functional). *Let $\nu \in \mathcal{P}(\overline{\mathbb{B}}(0, 1))$ and $r > \sqrt{d}$. For any $\mu_0 \in \mathcal{P}(\overline{\mathbb{B}}(0, r))$ with a density $\rho_0 \in L^\infty(\overline{\mathbb{B}}(0, r))$ and $h > 0$, there exists a $\hat{\mu} \in \mathcal{P}(\overline{\mathbb{B}}(0, r))$ that minimizes the following functional:*

$$\mathcal{G}(\mu) = \mathcal{F}_{\lambda,\sigma}^\nu(\mu) + \frac{1}{2h} \mathcal{W}_2^2(\mu, \mu_0), \quad (36)$$

where $\mathcal{F}_{\lambda,\sigma}^\nu(\mu)$ is given by (12). Moreover $\hat{\mu}$ admits a density $\hat{\rho}$ on $\overline{\mathbb{B}}(0, r)$.

Proof. We note that $\mathcal{P}(\overline{\mathbb{B}}(0, 1))$ is compact for weak convergence (and equivalently for convergence in W_2). Hence, showing that $\mathcal{G}(\mu)$ is lower semi-continuous on $\mathcal{P}(\overline{\mathbb{B}}(0, 1))$ would suffice to show the existence of a solution $\hat{\mu}$. By Lemma 9.4.3 of [Ambrosio \(2008\)](#), \mathcal{H} is lower semi-continuous. By [Rakotomamonjy & Ralaivola \(2021\)](#), $\mathcal{G}_{\sigma}\mathcal{SW}_2(\mu, \nu)$ is symmetric and satisfies the triangle inequality. Moreover, $\mathcal{G}_{\sigma}\mathcal{SW}_2(\mu, \nu) \leq \mathcal{SW}_2(\mu, \nu)$ for any $\sigma \geq 0$. Hence for any $\xi, \xi' \in \mathcal{P}(\overline{\mathbb{B}}(0, 1))$,

$$|\mathcal{G}_{\sigma}\mathcal{SW}_2(\xi, \nu) - \mathcal{G}_{\sigma}\mathcal{SW}_2(\xi', \nu)| \leq \mathcal{G}_{\sigma}\mathcal{SW}_2(\xi, \xi') \leq \mathcal{SW}_2(\xi, \xi') \leq c_d \mathcal{W}(\xi, \xi'),$$

where $c_d > 0$ is a constant only dependent on the dimension d , and the last inequality follows from Proposition 5.1.3 in [Bonnotte \(2013\)](#). Hence, there exists a minimum $\hat{\mu} \in \mathcal{P}(\overline{\mathbb{B}}(0, r))$ of $\mathcal{G}(\mu)$. Moreover, $\hat{\mu}$ must admit a density $\hat{\rho}$ because otherwise $\mathcal{H}(\hat{\mu}) = \infty$. \square

Lemma 2 (Regularity of the solution to the minimizing functional). Under the assumptions of Theorem 3, any minimizer $\hat{\mu}$ of $\mathcal{G}(\mu)$ in (36) must admit a strictly positive density $\hat{\rho} > 0$ a.e., and $\|\hat{\rho}\|_{L^\infty} \leq (1 + h/\sqrt{d})^{\sqrt{d}} \|\rho_0\|_{L^\infty}$.

Proof. By Theorem 3, a minimizer $\hat{\mu}$ of $\mathcal{G}(\mu)$ exists and admits a density $\hat{\rho}$. Let $\bar{\mu} \in \mathcal{P}(\bar{\mathbb{B}}(0, 1))$ be an arbitrary probability measure with density $\bar{\rho}$. For $\varepsilon \in (0, 1)$ let $\rho_\varepsilon = (1 - \varepsilon)\hat{\rho} + \varepsilon\bar{\rho}$ and let $\mu_\varepsilon \in \mathcal{P}(\bar{\mathbb{B}}(0, 1))$ be the probability measure corresponding to the density ρ_ε . By the optimality of $\hat{\rho}$, we have that $\mathcal{G}(\hat{\mu}) \leq \mathcal{G}(\mu_\varepsilon)$. Hence,

$$\begin{aligned} 0 &\geq \lim_{\varepsilon \rightarrow 0^+} \frac{\mathcal{G}(\hat{\mu}) - \mathcal{G}(\mu_\varepsilon)}{\varepsilon} = \lim_{\varepsilon \rightarrow 0^+} \frac{\mathcal{G}_\sigma \mathcal{S} \mathcal{W}_2^2(\hat{\mu}) - \mathcal{G}_\sigma \mathcal{S} \mathcal{W}_2^2(\mu_\varepsilon)}{2\varepsilon} + \lambda \limsup_{\varepsilon \rightarrow 0^+} \frac{\mathcal{H}(\hat{\mu}) - \mathcal{H}(\mu_\varepsilon)}{\varepsilon} + \lim_{\varepsilon \rightarrow 0^+} \frac{\mathcal{W}_2^2(\hat{\mu}) - \mathcal{W}_2^2(\mu_\varepsilon)}{2h\varepsilon} \\ &= \int_{\mathbb{S}^{d-1}} \int_{\Omega} \psi_{\theta, \sigma}(\langle \theta, x \rangle) d(\bar{\mu} - \hat{\mu}) d\theta + \lambda \limsup_{\varepsilon \rightarrow 0^+} \frac{\mathcal{H}(\hat{\mu}) - \mathcal{H}(\mu_\varepsilon)}{\varepsilon} + \int_{\Omega} \phi d(\bar{\mu} - \hat{\mu}), \end{aligned}$$

where the last equality follows by combining Proposition 1 with Proposition 1.5.6 in (Bonnotte, 2013). Here, $\psi_{\theta, \sigma}$ is a Kantorovich potential between $\theta_{\#} \hat{\mu} * \mathcal{N}_\sigma$, and $\theta_{\#} \nu * \mathcal{N}_\sigma$ as in Proposition 1 and ϕ is a Kantorovich potential between $\hat{\mu}$ and ν for \mathcal{W}_2 . Rearranging, we get the following:

$$\limsup_{\varepsilon \rightarrow 0^+} \frac{\mathcal{H}(\hat{\mu}) - \mathcal{H}(\mu_\varepsilon)}{\varepsilon} \leq \frac{1}{\lambda} \int_{\bar{\mathbb{B}}(0, r)} \Psi d(\bar{\mu} - \hat{\mu}), \quad (37)$$

where $\Psi(x) := \int_{\mathbb{S}^{d-1}} \psi_{\theta, \sigma}(\langle \theta, x \rangle) + \frac{1}{h} \phi(x)$. From this point, for any $\mu_0 \in \mathcal{P}(\bar{\mathbb{B}}(0, r))$ with a density ρ_0 that is smooth and strictly positive, we get the desired result by following the proof strategy of Lemma 5.4.3 in (Bonnotte, 2013). For a more general μ_0 with a density $\rho_0 \in L^\infty(\bar{\mathbb{B}}(0, r))$, we again arrive at the desired result by following the proof strategy of Theorem S4 in (Liutkus et al., 2019), which proceeds by smoothing ρ_0 by convolution with a Gaussian. \square

Theorem 4 (Existence of GMMS). *Under the assumptions of Theorem 3, there exists a GMMS $(\mu_t)_{t \geq 0}$ in $\mathcal{P}(\bar{\mathbb{B}}(0, r))$, starting from μ_0 for the following functional:*

$$\mathcal{F}_{\lambda, \sigma}^\nu(h, \mu_{nxt}, \mu_{prv}) = \mathcal{F}_{\lambda, \sigma}^\nu(\mu_{nxt}) + \frac{1}{2h} \mathcal{W}_2^2(\mu_{nxt}, \mu_{prv}). \quad (38)$$

Moreover, for any $t > 0$, μ_t has a density ρ_t such that $\|\rho_t\|_{L^\infty} \leq e^{td\sqrt{d}} \|\rho_0\|_{L^\infty}$.

Proof. The desired result follows straightforwardly by following the proof of Theorem S5 in Liutkus et al. (2019) or Theorem 5.5.3 in Bonnotte (2013), with the support of Lemma 2 and Theorem 3. \square

Theorem 5 (Continuity equation for GMMS). *Under the assumptions of Theorem 3, let $(\mu_t)_{t \geq 0}$ be the GMMS given by Theorem 4. For $\theta \in \mathbb{S}^{d-1}$, let $\psi_{t, \theta}^{(\sigma)}$ be the Kantorovich potential between $P_{\#}^\theta \mu_t * \xi_\sigma$ and $P_{\#}^\theta \nu * \xi_\sigma$, with $\xi_\sigma \sim \mathcal{N}(0, \sigma^2)$. For $t \geq 0$, the density ρ_t of μ_t satisfies the following continuity equation in a weak sense:*

$$\frac{\partial \rho_t}{\partial t} = -\operatorname{div}(v_t^{(\sigma)} \rho_t) + \lambda \Delta \rho_t,$$

with:

$$v_t^{(\sigma)}(x) = v^{(\sigma)}(x, \mu_t) = \int_{\mathbb{S}^{d-1}} (\psi_{t, \theta}^{(\sigma)})'(\langle x, \theta \rangle) \theta d\theta.$$

That is, for all $\xi \in C_c^\infty([0, \infty) \times \bar{\mathbb{B}}(0, r))$,

$$\int_0^\infty \int_{\bar{\mathbb{B}}(0, r)} \left[\frac{\partial \xi}{\partial t}(t, x) - v_t^{(\sigma)} \nabla \xi(t, x) - \lambda \Delta \xi(t, x) \right] \rho_t(x) dx dt = - \int_{\bar{\mathbb{B}}(0, r)} \xi(0, x) \rho_0(x) dx. \quad (39)$$

Proof. We will closely follow the proof of Theorem S6 in Liutkus et al. (2019) and Theorem 5.6.1 in Bonnotte (2013). Just as in the proof of Theorem S6 in Liutkus et al. (2019), we will proceed in five steps.

Step (1): By the definition of GMMS, there exists a family of piecewise constant trajectories $(\mu^{h_n})_{n \in \mathbb{N}}$ for $\mathcal{F}_{\lambda, \sigma}^\nu$ such that $\lim_{n \rightarrow \infty} \mu^{h_n} = \mu_t$ for all $t \in \mathbb{R}_+$. Let $\xi \in C_c^\infty([0, \infty) \times \bar{\mathbb{B}}(0, r))$ and let $\xi_k^n(x)$ denote $\xi(kh_n, x)$. Using step 1 of the proof of Theorem S6 in Liutkus et al. (2019), we get:

$$\int_{\bar{\mathbb{B}}(0, r)} \xi(0, x) \rho_0(x) dx + \int_0^\infty \int_{\bar{\mathbb{B}}(0, r)} \frac{\partial \xi}{\partial t}(t, x) \rho_t(x) dx dt = \lim_{n \rightarrow \infty} -h_n \sum_{k=1}^\infty \int_{\bar{\mathbb{B}}(0, r)} \xi_k^n(x) \frac{\rho_{kh_n}^{h_n}(x) - \rho_{(k-1)h_n}^{h_n}(x)}{h_n} dx. \quad (40)$$

Step (2): For any $\theta \in \mathbb{S}^{d-1}$, let $\psi_{t,\theta}^{(\sigma),h_n}$ be the Kantorovich potential between $P_{\#}^{\theta} \mu_t^{h_n} * \xi_{\sigma}$ and $P_{\#}^{\theta} \nu * \xi_{\sigma}$, with $\xi_{\sigma} \sim \mathcal{N}(0, \sigma^2)$. Using step 2 of the proof of Theorem S6 in Liutkus et al. (2019), we get:

$$\int_0^{\infty} \int_{\overline{\mathbb{B}}(0,r)} \int (\psi_{t,\theta}^{(\sigma)})'(\langle \theta, x \rangle) \langle \theta, \nabla \xi(x,t) \rangle d\theta d\mu_t(x) dt = \lim_{n \rightarrow \infty} h_n \sum_{k=1}^{\infty} \int_{\overline{\mathbb{B}}(0,r)} \int \psi_{kh_n,\theta}^{(\sigma),h_n}(\theta^*) \langle \theta, \nabla \xi_k^n \rangle d\theta d\mu_{kh_n}^{h_n}. \quad (41)$$

Step (3): From step 3 of the proof of Theorem S6 in Liutkus et al. (2019), we get:

$$\lim_{n \rightarrow \infty} h_n \sum_{k=1}^{\infty} \int_{\overline{\mathbb{B}}(0,r)} \Delta \xi_k^n(x) \rho_{kh_n}^{h_n}(x) dx = \int_0^{\infty} \int_{\overline{\mathbb{B}}(0,r)} \Delta \xi(t,x) \rho_t(x) dx dt. \quad (42)$$

Step (4): Let $\phi_k^{h_n}$ be the Kantorovich potential from $\mu_{kh_n}^{h_n}$ to $\mu_{(k-1)h_n}^{h_n}$. From the optimality of $\mu_{kh_n}^{h_n}$, the first variation of the functional $\zeta \mapsto \mathcal{F}_{\lambda,\sigma}^{\nu}(\zeta) + \frac{1}{2h} \mathcal{W}_2^2(\zeta, \mu_{kh_n}^{h_n})$ with respect to ζ at the point $\mu_{kh_n}^{h_n}$ in the direction of the vector field $\nabla \xi_k^n$ is zero. Using Proposition 2 for the first variation of the $\mathcal{G}_{\sigma} \mathcal{S} \mathcal{W}_2^2$ term, Proposition 5.1.7 for the first variation of the \mathcal{W}_2^2 term, and Jordan et al. (1996) for the first variation of the \mathcal{H} term, we get the following:

$$0 = \frac{1}{h_n} \int_{\overline{\mathbb{B}}(0,r)} \langle \nabla \phi_k^{h_n}(x), \nabla \xi_k^n(x) \rangle d\mu_{kh_n}^{h_n}(x) - \int_{\overline{\mathbb{B}}(0,r)} \int (\psi_{kh_n,\theta}^{(\sigma),h_n})'(\theta^*) \langle \theta, \nabla \xi_k^n(x) \rangle d\theta d\mu_{kh_n}^{h_n}(x) - \lambda \int_{\overline{\mathbb{B}}(0,r)} \Delta \xi_k^n(x) d\mu_{kh_n}^{h_n}(x). \quad (43)$$

Proceeding as in step 4 of Liutkus et al. (2019) and using (43), we get the following:

$$\begin{aligned} & \lim_{n \rightarrow \infty} -h_n \sum_{k=1}^{\infty} \xi_k^n(x) \frac{\rho_{kh_n}^{h_n} - \rho_{(k-1)h_n}^{h_n}}{h_n} dx \\ &= \lim_{n \rightarrow \infty} \left(h_n \sum_{k=1}^{\infty} \int_{\overline{\mathbb{B}}(0,r)} \int (\psi_{kh_n,\theta}^{(\sigma),h_n})'(\theta^*) \langle \theta, \nabla \xi_k^n \rangle d\theta d\mu_{kh_n}^{h_n} + h_n \sum_{k=1}^{\infty} \int_{\overline{\mathbb{B}}(0,r)} \Delta \xi_k^n(x) \rho_{kh_n}^{h_n}(x) dx \right). \end{aligned} \quad (44)$$

Step (4): Combining (40), (41), (42) and (44), we get the desired result in (39). □

B PROOF OF THEOREM 2

We simply follow the proof strategy of Theorem 3 in Liutkus et al. (2019). We begin by restating the following two discrete-time SDEs:

$$\widehat{X}_{k+1} = hv^{(\sigma)}(\widehat{X}_k, \widehat{\mu}_{kh}) + \sqrt{2\lambda h} Z_{k+1}, \quad (45)$$

$$\bar{X}_{k+1} = h\widehat{v}^{(\sigma)}(\bar{X}_k, \bar{\mu}_{kh}) + \sqrt{2\lambda h} Z_{k+1}, \quad (46)$$

where (45) is equivalent to (17), which in turn is the Euler-Maruyama discretization of the continuous-time SDE in (16). Equation 46 is equivalent to the particle update equation in (18).

Similar to the proof of Theorem 3 in Liutkus et al. (2019), we define two continuous-time processes $(Y_t)_{t \geq 0}$ and $(U_t)_{t \geq 0}$, defined by the following continuous-time SDEs:

$$dY_t = \tilde{v}_t^{(\sigma)}(Y) dt + \sqrt{2\lambda} dW_t, \quad (47)$$

$$dU_t = \tilde{v}_t^{(\sigma)}(U) dt + \sqrt{2\lambda} dW_t, \quad (48)$$

where

$$\tilde{v}_t(Y) := - \sum_{k=0}^{\infty} \widehat{v}_{kh}^{(\sigma)}(Y_{kh}, \widehat{\mu}_{kh}) \mathbf{1}_{[kh, (k+1)h)}(t), \quad (49)$$

$$\tilde{v}_t(U) := - \sum_{k=0}^{\infty} \widehat{v}_{kh}^{(\sigma)}(U_{kh}, \bar{\mu}_{kh}) \mathbf{1}_{[kh, (k+1)h)}(t). \quad (50)$$

In (49), $\hat{\mu}_{kh}$ follows the distribution of \widehat{X}_k in the discrete-time process defined by the update equation in (45). Therefore $(Y_t)_{t \geq 0}$ is a continuous linear interpolation of the discrete-time process $(\widehat{X}_k)_{k \in \mathbb{N}_+}$.

In (50), $\bar{\mu}_{kh}$ follows the distribution of \bar{X}_k in the discrete-time process defined by the update equation in (46). Therefore $(U_t)_{t \geq 0}$ is a continuous linear interpolation of the discrete-time process $(\bar{X}_k)_{k \in \mathbb{N}_+}$.

Let π_X^T , π_Y^T , and π_U^T denote the distributions of $(X_t)_{t \in [0, T]}$, $(Y_t)_{t \in [0, T]}$, and $(U_t)_{t \in [0, T]}$, respectively, with $T = Kh$. We have the following lemma bounding the total variation distance between the pairs (π_X^T, π_Y^T) and (π_Y^T, π_U^T) from Liutkus et al. (2019):

Lemma 3 (Lemmas S1 and S2 in Liutkus et al. (2019)). For all $\lambda > 0$, assume that the continuous-time SDE in (16) has a unique strong solution $(X_t)_{t \geq 0}$ for any starting point $x \in \mathbb{R}^d$. For $t \geq 0$, define $\Psi_t^{(\sigma)}(x) := \int_{\mathbb{S}^{d-1}} \psi_{t, \theta}^{(\sigma)}(\langle \theta, x \rangle) d\theta$. Suppose there exists constants $A, B, L, m, b > 0$, and $\delta \in (0, 1)$, such that the following are true for any $x, x' \in \mathbb{R}^d$, $\mu, \mu' \in \mathcal{P}(\Omega)$, and all $t \geq 0$:

$$\begin{aligned} \|v_t^{(\sigma)}(x) - v_t^{(\sigma)}(x')\| &\leq L(\|x - x'\| + |t - t'|), \\ \|\hat{v}^{(\sigma)}(x, \mu) - \hat{v}^{(\sigma)}(x', \mu')\| &\leq L(\|x - x'\| + \|\mu - \mu'\|_{\text{TV}}), \\ \langle x, v_t^{(\sigma)}(x) \rangle &\geq m\|x\|^2 - b, \\ \mathbb{E}[\hat{v}_t^{(\sigma)}] &= v_t^{(\sigma)}, \\ \mathbb{E}[\|\hat{v}^{(\sigma)}(x, \mu_t) - v^{(\sigma)}(x, \mu_t)\|^2] &\leq 2\delta(L^2\|x\|^2 + B^2). \end{aligned}$$

Define:

$$\begin{aligned} C_e &:= \mathcal{H}(\mu_0), \\ C_0 &:= C_e + 2(1 \vee \frac{1}{m})(b + 2B^2 + d\lambda), \\ C_1 &:= 12(L^2C_0 + B^2) + 1, \\ C_2 &:= 2(L^2C_0 + B^2). \end{aligned}$$

Then, we have:

$$\begin{aligned} \|\pi_X^T - \pi_Y^T\|_{\text{TV}}^2 &\leq \frac{L^2K}{4\lambda} \left(\frac{C_1h^3}{3} + 3\lambda dh^2 \right) + \frac{C_2\delta Kh}{8\lambda}, \\ \|\pi_Y^T - \pi_U^T\|_{\text{TV}}^2 &\leq \frac{L^2Kh}{16\lambda} \|\pi_X^T - \pi_U^T\|_{\text{TV}}^2. \end{aligned}$$

Theorem 6. Under the assumptions of Lemma 3 and for $\lambda > TL_\sigma^2/8$:

$$\|\mu_T - \hat{\mu}_{Kh}\|_{\text{TV}}^2 \leq \frac{T}{\lambda - TL_\sigma^2/8} \left[L_\sigma^2 h(c_1h + d\lambda) + c_2\delta \right], \quad (51)$$

where $c_1, c_2, L_\sigma, \delta > 0$ are constants independent of time.

Proof. We will emulate the proof of Theorem 3 in Liutkus et al. (2019).

$$\begin{aligned} \|\pi_X^T - \pi_U^T\|_{\text{TV}}^2 &\leq 2\|\pi_X^T - \pi_Y^T\|_{\text{TV}}^2 + 2\|\pi_Y^T - \pi_U^T\|_{\text{TV}}^2 \\ &\leq \frac{L^2K}{2\lambda} \left(\frac{C_1h^3}{3} + 3\lambda dh^2 \right) + \frac{C_2\delta Kh}{4\lambda} + \frac{L^2Kh}{8\lambda} \|\pi_X^T - \pi_U^T\|_{\text{TV}}^2 \\ &\leq \left(1 - \frac{KL^2h}{8\lambda} \right)^{-1} \left\{ \frac{L^2K}{2\lambda} \left(\frac{C_1h^3}{3} + 3\lambda dh^2 \right) + \frac{C_2\delta Kh}{4\lambda} \right\}, \end{aligned}$$

where the second inequality follows from Lemma 3 and the last inequality holds for $\lambda > TL_\sigma^2/8$. The desired result then follows by plugging in $T = Kh$ and rearranging. \square

C EXPERIMENTAL DETAILS

In this section, we explain all experimental details required running the experiments (along with the code which is provided in the supplementary material). For this projects we use 1 GPU Tesla V100 which was necessary for the pretraining of the auto-encoder only.

C.1 Structure of the Autoencoders for Data Dimension Reduction

The experiments performed on MNIST and FashionMNIST datasets utilize an autoencoder architecture as per the framework proposed by Liutkus et al. (2019). Furthermore, we normalized the latent space before adding Gaussian noise, ensuring that the encoded representations lie on a hyper-sphere. We use the following autoencoder structure, which is the same as that used in Liutkus et al. (2019):

- **Encoder.** Four 2d convolution layers with (num chan out, kernel size, stride, padding) set to (3, 3, 1, 1), (32, 4, 2, 0), (32, 3, 1, 1), (32, 3, 1, 1), each one followed by a ReLU activation. At the output, a linear layer is set to the desired bottleneck size, and then the outputs are normalized.
- **Decoder.** A linear layer receives from the bottleneck features a vector of dimension 8192, which is reshaped as (32, 16, 16). Then, three convolution layers are applied, all with 32 output channels and (kernel size, stride, panning) set to, respectively, (3, 1, 1), (3, 1, 1), (2, 2, 0). A 2d convolution layer is then applied, with the specified output number of channels set to that of the data (1 for black and white, 3 for color), and a (kernel size, stride, panning) set to (3, 1, 1). All layers are followed by a ReLU activation, and a sigmoid activation is applied to the final output.

Conversely, experiments conducted on the CelebA dataset employ an autoencoder/generator architecture based on the DCGAN framework proposed by Radford et al. (2016). The structure is the following:

- **Encoder.** Four 2D convolution layers are employed with the following specifications: (64,3,1,1), (64*2,4,2,1), (64*4,4,2,1) and (64*8,4,2,1). Each convolutional layer is followed by a leaky Rectified Linear Unit (LeakyReLU) activation function. Subsequently, a linear layer is applied to obtain the desired bottleneck size. The outputs are then normalized.
- **Decoder.** Four 2D convolution layers are employed with the following specifications: (64*8,4,1,0), (64*4,4,2,1), (64*2,4,2,1) and (64,4,2,1). Each convolutional layer is followed by a leaky Rectified Linear Unit (LeakyReLU) activation function and batch normalization is added after the activation.

C.2 DPSWflow

DPSWflow (Algorithm 2) is a variant of DPSWflow-r that omits re-sampling of the projections θ at each step of the flow. Instead, we generate N_θ random directions $\theta_n \sim \text{Uniform}(S^{d-1})$ and store them in the vector Θ . During each iteration of the flow, we subsample M_θ random directions from Θ , where $M_\theta < N_\theta$. This introduces an element of randomness that has demonstrated improved output results. Importantly, this randomness is incorporated without incurring any additional cost, as we take into account N_θ for the privacy guarantee computation.

C.3 Additional Comments on Hyperparameters for Experiments conducted on MNIST and FashionMNIST

In this subsection we give all of the hyperparameters necessary for reproducing the experiments conducted on MNIST and FashionMNIST. All three evaluated methods, DPSWflow, DPSWflow-r, and DPSWgen are evaluated with a batch size of 250 and for $\delta = 10^{-5}$. DPSWflow is evaluated over 1500 epochs for all values of ε , while DPSWflow-r and DPSWgen are evaluated on 35 epochs for $\varepsilon = \infty$ and $\varepsilon = 10$, and on 20 epochs for $\varepsilon = 5$. DPSWflow uses $N_\theta = 31$ and $M_\theta = 25$, while DPSWflow-r and DPSWgen use $N_\theta = 70$. As explained in Section 5.2, the privacy track is different for DPSWflow compared to DPSWflow-r and DPSWgen. For DPSWflow we directly input the desired value for ε and use the sensitivity bound from Equation 26, along with $\sigma \geq c \frac{\Delta_2(f)}{\varepsilon}$ (from Section 2.1), to obtain the value of σ which is used in our code. For DPSWflow-r and DPSWgen we used the following pairs of σ, ε : $\sigma = 0, \varepsilon = \infty$; $\sigma = 0.68, \varepsilon = 10$; and $\sigma = 0.9, \varepsilon = 5$.

Algorithm 2: Differentially Private Sliced Wasserstein Flow without resampling of the θ s: DPSWflow

Input: $Y = [Y_1^T, \dots, Y_n^T]^T \in \mathbb{R}^{n \times d}$ i.e. N i.i.d. samples from target distribution ν , number of projections N_θ , regularization parameter λ , variance σ , step size h .

Output: $\{\hat{X}_i\}_{i=1}^N$

```

// Initialize the particles
1  $\{\hat{X}_0^i\}_{i=1}^N \sim \mu_0, \hat{X} = [x_1^T, \dots, x_n^T]^T \in \mathbb{R}^{n \times d};$ 
2  $\{\theta_j\}_{j=1}^{N_\theta} \sim \text{Unif}(\mathbb{S}^{d-1}), \Theta = [\theta_1^T, \dots, \theta_{N_\theta}^T];$ 
3 Sample  $Z_Y \in \mathbb{R}^{n \times N_\theta}$  from i.i.d  $\mathcal{N}(0, \sigma^2)$ ;
4 Compute the quantiles of  $Y\Theta + Z_Y$ ;
// Iterations
5 for  $k = 0, \dots, K - 1$  do
6   Sample  $Z_X \in \mathbb{R}^{n \times N_\theta}$  from i.i.d.  $\mathcal{N}(0, \sigma^2)$ ;
7   Compute the CDF of  $X\Theta + Z_X$ ;
8   Compute  $\hat{v}^{(\sigma)}(\hat{X}_k^i)$  using (20) and (21);
9    $\hat{X}_{k+1}^i \leftarrow h\hat{v}^{(\sigma)}(\hat{X}_k^i) + \sqrt{2\lambda h}Z$ , where  $Z \sim \mathcal{N}(0, 1)$ .
```

Table 2: Summary of the FID results on the CelebA dataset for the two variants of our method.

	ε	∞	10	5
DPSWflow-r	57	134	202	
DPSWflow	134	262	292	

C.4 Datasets and Evaluation Metric

MNIST is a standard dataset introduced in [LeCun et al. \(1998\)](#), with no clear license to the best of our knowledge, composed of monochrome images of hand-written digits. Each MNIST image is single-channel, of size 28×28 . We preprocess MNIST images by extending them to 32×32 frames (padding each image with black pixels), in order to better fit as inputs and outputs of standard convolutional networks. MNIST is comprised of a training and testing dataset, but no validation set. We split the training set into two equally-sized public and private sets.

FashionMNIST is a similar dataset introduced by [Xiao et al. \(2017\)](#) under the MIT license, composed of fashion-related images. Each FashionMNIST image is single-channel, of size 28×28 , and we also preprocess them by extending them to 32×32 frames. Like MNIST, FashionMNIST is comprised of a training and testing dataset, but no validation set. We split the training set into two equally-sized public and private sets.

CelebA is a dataset composed of celebrity pictures introduced by [Liu et al., 2015](#)). Its license permits use for non-commercial research purposes. Each CelebA image has three color channels, and is of size 178×218 . We preprocess these images by center-cropping each to a square image and resizing to 64×64 with a Lanczos filter. CelebA is comprised of a training, testing, and validation dataset. After conducting initial experiments and analysis with the validation set, we removed it. We then split the training set into two equally-sized public and private datasets.

Fréchet Inception Distance (FID) was introduced by [Heusel et al. \(2018\)](#). It measures the generative performance of the models we consider. In our code we use the PyTorch implementation of TorchMetrics.

D ADDITIONAL RESULTS

We conducted more experiments on CelebA ([Liu et al., 2015](#)). Both the DPSWflow and DPSWflow-r methods are evaluated with a batch size of 250 and for $\delta = 10^{-6}$. DPSWflow is evaluated over 2000 epochs for every value of ε , while DPSWflow-r is evaluated on 30 epochs for every ε . DPSWflow uses $N_\theta = 250$ and $M_\theta = 220$, while DPSWflow-r uses $N_\theta = 300$. For DPSWflow-r we used the following pairs of σ, ε : $\sigma = 0, \varepsilon = \infty$; $\sigma = 0.59, \varepsilon = 10$; and $\sigma = 0.8, \varepsilon = 5$. We give the results of these experiments in Table 2 and Figure 3.



Figure 3: Examples of images generated with our DPSWflow-r method. The first image one is for no DP ($\varepsilon = \infty$), the middle one is for $\varepsilon = 10$, and the third one is for $\varepsilon = 5$.